Ductile Gas Barrier Poly(ester-amide)s Derived from Glycolide

Yoon-Jung Jang, Leire Sangroniz, and Marc Hillmyer*

*Department of Chemistry, University of Minnesota, Minneapolis, MN55455-0431

*Corresponding author (e-mail:hillmyer@umn.edu)

Abstract

Sustainable gas barrier materials, such as polyglycolide, poly(L-lactide), and poly(ethylene 2,5-furandicarboxylate) are important alternatives to traditional plastics used for packaging where low gas permeability is beneficial. However, high degrees of crystallinity in these materials can lead to undesirably low material toughness. We report poly(ester-amide)s derived from glycolide and diamines exhibiting both high toughness and desirable gas barrier properties. These sustainable poly(ester-amide)s were synthesized from glycolide-derived diamidodiols and diacids. To understand the structure–property relationships of the poly(ester-amide)s, polymers with different numbers of methylene groups were compared with respect to thermal, mechanical, and gas barrier properties. As the number of methylene groups between ester groups increased in the even-numbered series, the melting temperature decreased and oxygen permeability increased. We also found that these polymers are readily degradable under neutral, acidic, and basic hydrolytic conditions. These high-performance poly(ester-amide)s are promising sustainable alternatives to conventional gas barrier materials.

TOC graphic

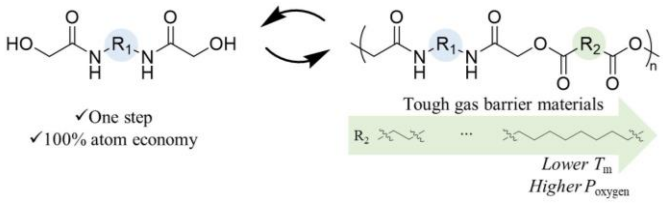

Introduction

Gas barrier materials are widely used in packaging for food, cosmetic, and pharmaceutical products. Specifically, the global food packaging market size is expected to reach over 400 billion US dollars by 2025.[1] Plastic packaging extends the shelf life of products by protecting them from oxygen and moisture in transportation and storage.[2] To obtain these benefits, gas barrier materials require both mechanical toughness and low gas permeability for oxygen and water vapor. Based on these requirements, the dominant polymers used in packaging materials are ethylene vinyl alcohol (EVOH), poly(ethylene terephthalate) (PET), poly(vinylidene dichloride) (PVDC), polyethylene (PE), and polypropylene (PP), but these plastics are derived from nonrenewable resources (Chart 1A).[3–6] Furthermore, most packaging materials are not easily recycled after a single use because of typically multi-layered structures and, in many cases, contamination from the food they contain. These plastics are also not degradable on reasonable time scales in the natural environment or in engineered industrial composting facilities.[7–9] Since petroleum is a finite feedstock and plastic waste is accumulating in the environment, it is important to develop renewable and degradable alternatives.[10–12]

Chart 1. (A) Poly(ethylene terephthalate) (PET), (B) Polyglycolide (PGA), and (C) Poly(ester-amide)s

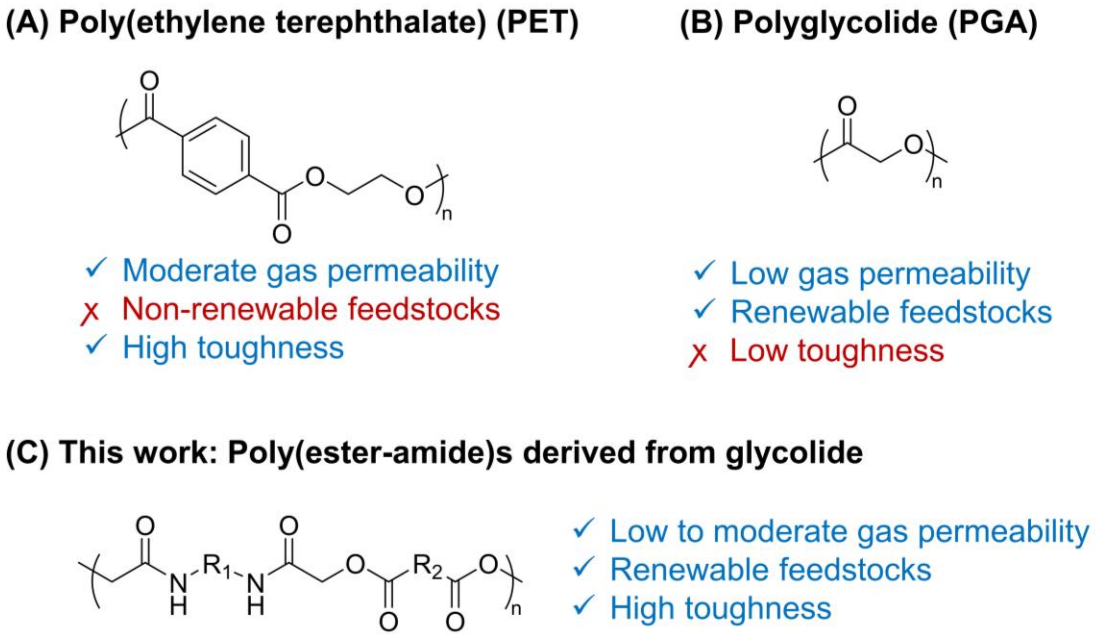

Sustainable gas barrier materials such as polyglycolide (PGA), polylactide (PLA), poly(ethylene 2,5-furandicarboxylate) (PEF), and poly(butylene succinate) (PBS) have gained attention because they are synthesized from renewable monomers and have been advanced as biodegradable materials.[1,13–25] However, most of them have not yet achieved the low gas permeabilities of commercial incumbents such as EVOH and PET. Polyglycolides, one of the most promising classes of gas barrier materials, have low gas permeability because of their typically high degrees of crystallinity and low free volume caused by intermolecular dipole-dipole interactions leading to high density (Chart 1B).[26,27] However, high crystallinity and low free volume can also undesirably contribute to brittleness and small difference between decomposition and melting temperatures. We recently reported the synthesis of glycolide copolymers to reduce the crystallinity to improve thermal processing windows without losing gas barrier properties, but

the copolymers still exhibited somewhat brittle characteristics.[28] Thus, gas barrier materials with both sustainability and ductility attributes are important targets.

Compared to polyesters, poly(ester-amide)s feature improved toughness and gas barrier characteristics by leveraging interchain hydrogen bonds between backbone amides while retaining hydrolytic degradability of polyesters.[29–32] As an example, Gao et al. improved mechanical and gas barrier properties of PET by copolymerizing 1,6-hexylenediamine and oligomers of PET.[33] One promising approach to preparing poly(ester-amide)s is through the step-growth polymerization of lactone-derived diamidodiols with diacids.[34–40] For example, caprolactones and valerolactones were used to generate poly(ester-amide)s, as reported by the groups of Feijin and Hoye.[35,38] Although these poly(ester-amide)s had ductile mechanical properties, with ultimate strains up to over 600% in some cases, their gas barrier characteristics were still in need of improvement.[39,40] In 2005, Vera et al. reported inspiring work that poly(ester-amide)s containing glycolate were degradable in enzymatic media and hydrolytic conditions.[41–44] Since materials containing glycolate units typically exhibit low gas permeability, we anticipated that these degradable poly(ester-amide)s derived from glycolide would have both promising mechanical and gas barrier properties (Chart 1C).

To this end, we synthesized a series of diamidodiols with 100% atom economy from glycolide and diamines. Glycolide can be prepared from sugarcanes, and 1,6-diaminohexane can be prepared from biosynthesis.[45,46] We then employed polycondensation reactions of these diamidodiols and diacids to generate poly(ester-amide)s. The thermal and mechanical properties of the resultant polymers were characterized using thermogravimetric analysis (TGA), differential scanning calorimetry (DSC), and tensile testing. The melting temperature depended on the number of methylene groups in the polymer repeat units. We investigated the gas permeability and

degradability of selected polymers based on thermal and mechanical properties and found that these sustainable polymers are useful gas barrier materials.

Results and Discussion

Synthesis of monomers

In previous studies, *N,N′*-(hexane-1,6-diyl)bis(2-hydroxyacetamide) (6G) was synthesized using glycolic acid and 1,6-diaminohexane in isopropanol.[37] To synthesize the 6G in a greener way, we prepared the monomer from 1,6-diaminohexane and glycolide under solvent-free conditions with perfect atom economy inspired by the synthesis reported by Lips et al., Stapert et al., and Vera et al. (Figure 1).[35,36,38] Under stoichiometrically balanced conditions, after the initial ring-opening of glycolide by the diamine, the unreacted amine groups reacted with the ester group of the intermediate to obtain 6G. At a reaction temperature of 60 °C on a 100 g scale in a 500 ml round bottom flask, the solventless reaction mixture became solid in 7 min after complete addition of glycolide. Near quantitative conversion (98%) was achieved in 30 min, as determined by ^{1}H NMR spectroscopy. The resulting product was obtained in pure form by recrystallization from an acetone/water mixture in high isolated yields (75%) and was analyzed by single-crystal X-ray diffraction (Figure 1). The analogous compounds 2G and 4G were also prepared in high yields using this scalable synthetic method utilizing 1,2-diaminoethane and 1,4-diaminobutane, respectively (Figure 1).

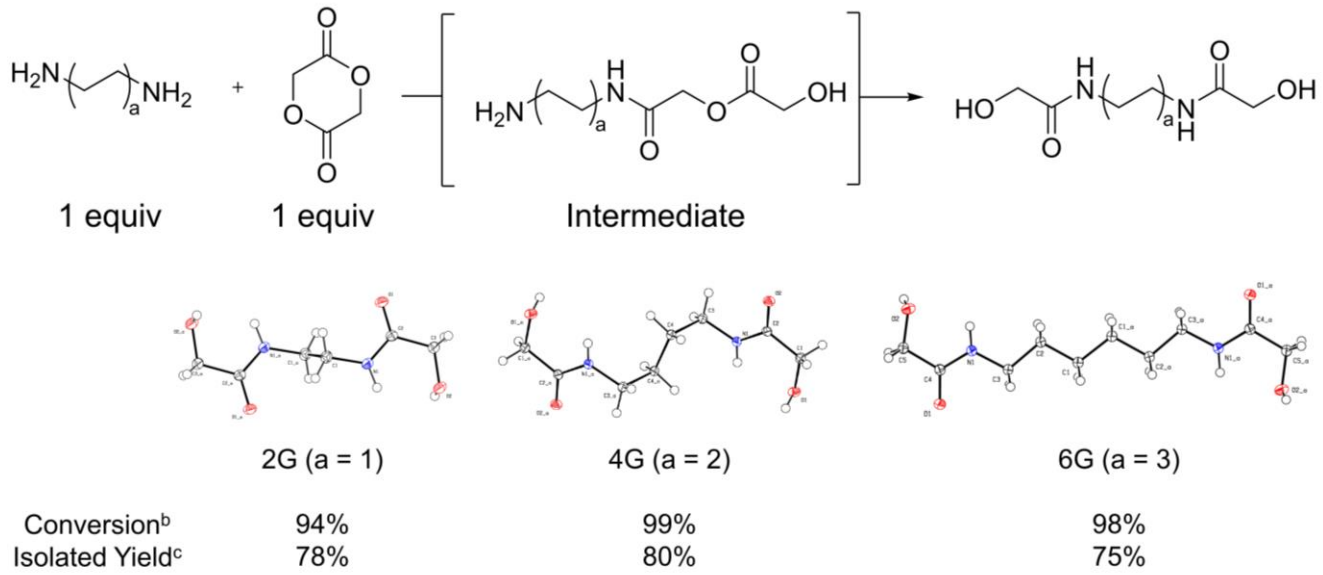

Figure 1. Synthesis of 2G, 4G, and 6G performed at room temperature, 40 °C, and 60 °C, respectively. [b]Conversions of diamines determined by ^{1}H NMR spectroscopy. [c]Isolated yields obtained by recrystallization from acetone/water; these crystalline products were characterized by X-ray crystallography.

Synthesis of poly(ester-amide)s

With 2G, 4G, and 6G monomers in hand, traditional condensation polymerizations were optimized to prepare high molar mass poly(ester-amide)s (Table S1). We attempted the melt polymerization of 6G and dimethyl adipate with various catalysts to synthesize 6G-4, having 6 methylene units between amide groups and 4 methylene units between ester groups. However, the yields were consistently low presumably due to low reactivity of 6G. The low reactivity of the monomer has also been reported in previous studies by Stapert et al.[36] Adipoyl chloride was used to increase the reactivity of comonomer, resulting in 6G-4 with the apparent number-average molar mass (M_n) of 7.8 kg/mol according to size-exclusion chromatography (SEC) in 1,1,1,3,3,3-hexafluoro isopropanol (HFIP) relative to PMMA standards.[37] However, the SEC trace was broad

and asymmetric, suggesting possible cross-linking from the amide group and acyl chloride (Figure S1). To reproducibly synthesize well-defined linear poly(ester-amide)s, we ultimately turned to using adipic acid with the 1-ethyl-3-(3-dimethylaminopropyl)carbodiimide (EDC) coupling reagent, resulting in 6G-4 with a relative M_n of 14 kg/mol in high isolated yields (79%). The dispersity for this sample was 1.9, which is close to the expected value for step-growth polymerization, implying minimal cross-linking and side reactions (Figure 2D).

The chemical structure of 6G-4 was characterized by ^{1}H NMR, ^{13}C NMR, and FTIR spectroscopies (Figure 2). The methylene peaks in the ^{1}H NMR and ^{13}C NMR spectra were consistent with the anticipated structures (Figure 2A & 2B). Furthermore, ester and amide carbonyl resonances were apparent in ^{13}C NMR spectrum. The carbonyl groups and N-H peak in the secondary amide were also analyzed by IR spectrum (Figure 2C). These data supported the chemical structure of 6G-4 synthesized through EDC coupling reaction as depicted in Figure 2.

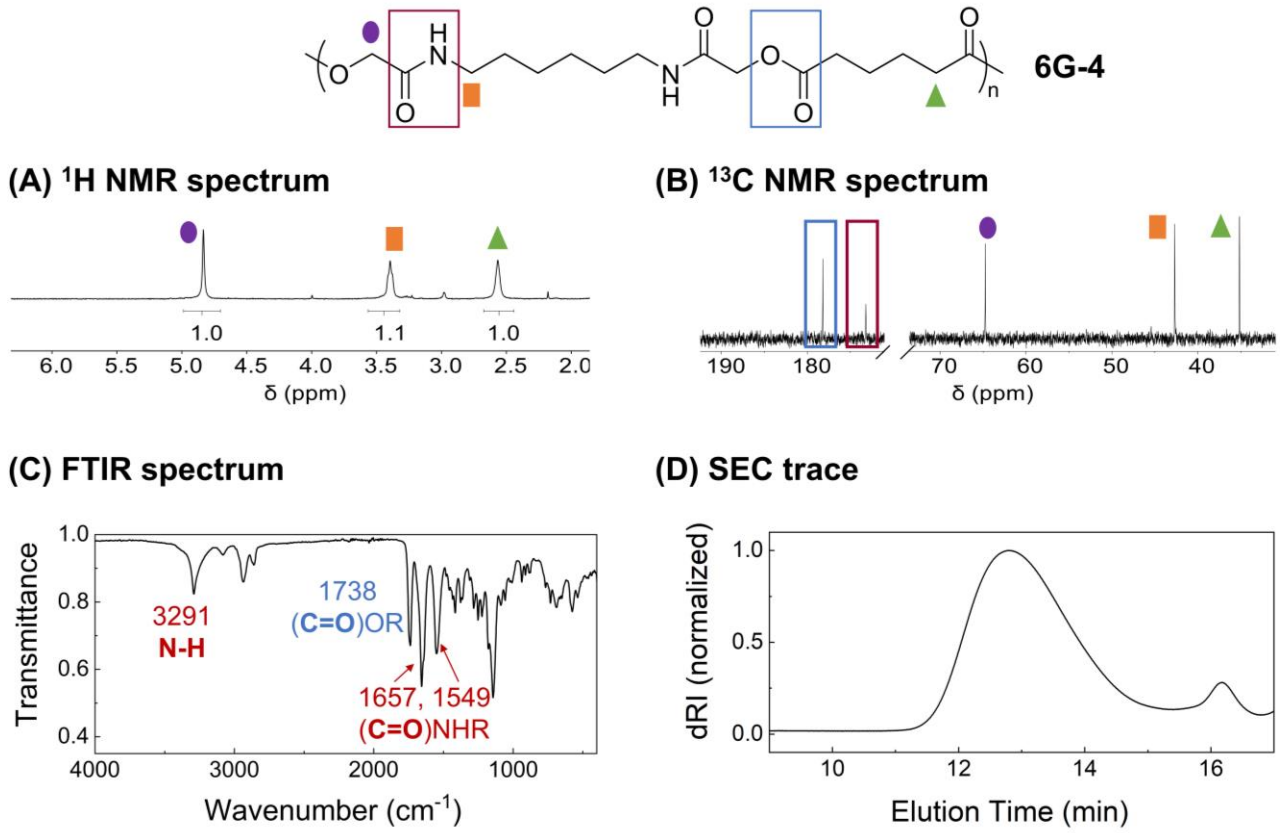

Figure 2. (A) ^{1}H NMR spectrum (TFA-*d*, 400 MHz) of 6G-4. (B) ^{13}C NMR spectrum (TFA-*d*, 100 MHz) of 6G-4. (C) FTIR spectrum of 6G-4 from the polymerization of 6G and adipic acid. (D) Normalized SEC trace; the peak at 16 min is presumably from cyclic oligomers. Polymerizations of 6G and adipic acid were performed with EDC·HCl and DMAP in DCM at room temperature for 1 day.

We then expanded the scope of poly(ester-amide)s to study the role of the alkyl chain lengths on polymer properties. Initially, we fixed the number of methylene groups between amide groups (x = 6) and varied the number of methylene groups between ester groups (y) from 2 to 8. Then, with a fixed alkyl chain length between ester groups (y = 4), the number of methylene groups between amide groups (x) was varied from 2 to 6. The polymerizations yielded poly(ester-amide)s with relative M_n values ranging from 14 to 32 kg/mol in the first series (variable y) and from 11 to 31 kg/mol in the second series (variable x, Table 1). The dispersity values for the poly(ester-

amide)s ranged from 1.8 to 2.4. Presumably, the higher apparent molar masses of 6G-5, 6G-8, and 2G-4 samples are due to higher solubility of these poly(ester-amide)s under the reaction conditions.

Table 1. Synthesis of Poly(ester-amide)s with Varying the Number of Methylene Groups between Amide and Ester Groups.

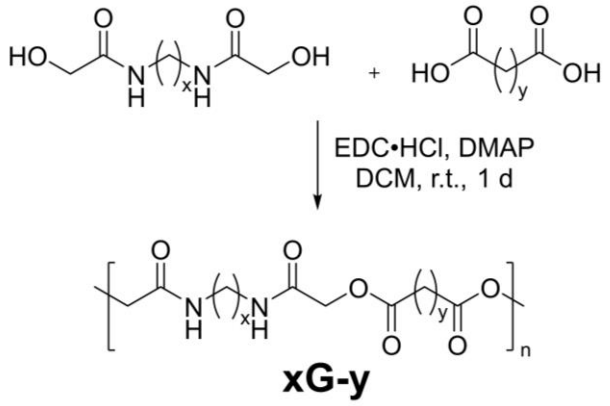

Entry	Polymer	x	y	M_n[a] (kg/mol)	M_w[a] (kg/mol)	$Đ$[a]
1	6G-2	6	2	15	31	2.1
2	6G-3	6	3	19	46	2.4
3	6G-4	6	4	14	27	1.9
4	6G-5	6	5	27	51	1.9
5	6G-6	6	6	16	30	1.9
6	6G-8	6	8	32	67	2.1
7	2G-4	2	4	31	74	2.4
8	4G-4	4	4	11	20	1.8

[a]Determined by HFIP SEC (0.025 M KTFA) at 40 °C calibrated by using PMMA standards.

Thermal properties of poly(ester-amide)s

The thermal properties of poly(ester-amide)s were studied by TGA and DSC. The polymers showed high thermal stability with high thermal decomposition temperatures (defined here as 5% mass loss, $T_{d,5\%}$) ranging from 255 to 344 °C under a nitrogen atmosphere (Table 2). The first DSC heating cycles were investigated for both dried precipitate powders and films obtained by solvent casting from HFIP using a tape coater. Poly(ester-amide) films had glass transition temperatures

(T_g) ranging from 44 to 53 °C from the first heating cycle, with a heating rate of 10 °C/min. Furthermore, poly(ester-amide)s films showed semi-crystallinity with melting temperatures (T_m) ranging from 99 to 187 °C and enthalpies of melting (ΔH_m) ranging from 36 to 59 J/g. Powder forms of poly(ester-amide)s had similar T_m but different ΔH_m values, presumably because the degree of crystallinity was influenced by the solvent casting procedure.[47] Although we used solvent casting to make films in this work, the width of the processing window ($T_{d,5\%} - T_m$) is important for future thermal processing to effectively reshape the polymers without decomposition concerns. The poly(ester-amide)s exhibited broad processing windows up to 236 °C which is much higher than that of PGA (≈ 75 °C).[28] Combined, these poly(ester-amide)s have T_g values higher than room temperature, semi-crystalline properties, and broad processing windows that render them promising candidates as packaging materials.

To investigate structure–thermal property relationships, we increased the number of methylene groups between ester groups (y), resulting in generally lower melting temperatures in a given series (Figure 3, filled squares). Poly(ester-amide)s with odd numbers of methylene units showed lower melting temperatures than those with even numbers, in good agreement with general trends for polyesters.[48] Nomura et al. explained that the even–odd effect arose from closely packed polymer chains in even-numbered systems because local polarization was minimized due to opposed dipole moments in the crystal structure; in contrast, dipole moments were aligned in the same direction in odd-numbered systems.[48,49] A clear trend in T_m was not observed with the variations of x, suggesting there are multiple factors at play, including the effects of hydrogen bonding in the crystal structure (Figure 3). The even–odd effect was also observed during DSC cooling cycle. While the crystallization temperatures (T_c) of poly(ester-amide)s varied from 58 to 128 °C, 6G-3 and 6G-5 did not recrystallize upon cooling at 10 °C min^{-1} from the melt.

Table 2. Thermal Properties of Poly(ester-amide)s with Varying the Number of Methylene Groups between Amide and Ester Groups.

	Thermal Properties										
Polymer	$T_{d,5\%}$[a] (°C)	$T_{g,f}$[b] (°C)	$T_{m,f}$[b] (°C)	$\Delta H_{m,f}$[b] (J/g)	$T_{g,p}$[c] (°C)	$T_{m,p}$[c] (°C)	$\Delta H_{m,p}$[c] (J/g)	$T_{c,p}$[d] (°C)	$\Delta H_{c,p}$[d] (J/g)	$T_{d,5\%} - T_{m,p}$ (°C)	χ_c[e] (%)
6G-2	310	44	163	59	34	162	77	116	59	148	32
6G-3	329	45	128	55	37	133	80	ND[f]	ND[f]	196	34
6G-4	283	45	122	49	50	127	71	58	5.2	156	28
6G-5	340	45	99	36	20	104	73	ND[f]	ND[f]	236	16
6G-6	344	46	119	42	36	122	56	70	45	222	13
6G-8	335	45	117	55	44	116	59	67	38	219	14
2G-4	298	52	187	42	52	186	52	128	54	112	12
4G-4	255	53	121	41	44	123	59	ND[f]	ND[f]	132	27

[a]Temperature at 5% mass loss determined by TGA at a heating rate of 10 °C/min under N_2 atmosphere. [b]Determined by DSC analysis of films under N_2 atmosphere starting from -20 °C at a heating rate of 10 °C/min based on the first heating cycle. [c]Determined by DSC analysis of powders under N_2 atmosphere starting from -20 °C at a heating rate of 10 °C/min based on the first heating cycle. [d]Determined by DSC analysis of powders under N_2 atmosphere starting from -20 °C at a heating and cooling rate of 10 °C/min based on the first cooling cycle. [e]Degree of crystallinity was determined by WAXD analysis. [f]Not detected.

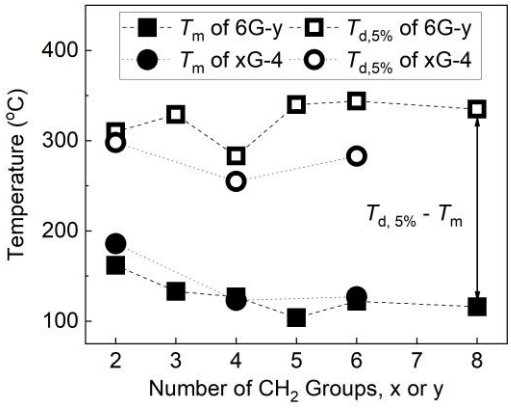

Figure 3. The effect of the number of methylene group on thermal properties of poly(ester-amide)s powders.

To study the effect of molar mass on thermal properties, 2G-4 samples with varying molar masses from 12 to 31 kg/mol were synthesized by adjusting reaction time (Table S2 & Figure S4). T_m ranged from 180 to 186 °C (Table S3 and Figure S5). T_c of 2G-4 with a relative M_n of 31 kg/mol was higher than that of 2G-4 with a lower molar mass. The higher T_c (128 °C) is presumably because 2G-4 (M_n = 31 kg/mol) crystals were incompletely melted after heating to 200 °C followed by immediate cooling. To investigate the effect of annealing time, 2G-4 was held at 200 °C for 3

min and 20 min in the first heating cycle in the DSC instrument, reducing the crystallization temperature in the cooling cycle to 75 °C and 53 °C, respectively (Figure S6). Annealing at higher temperature (260 °C) in DSC resulted in no evident crystallization peak in the cooling cycle (Figure S6).

Mechanical properties of poly(ester-amide)s

To investigate the mechanical properties of poly(ester-amide)s, films were solvent cast from HFIP using a tape casting coater and cut into dog-bone-shaped tensile bars. The samples of poly(ester-amide)s were subjected to uniaxial tensile tests, and the results are summarized in Figure 4 and Table S4; comparison to PGA and PET as commercially available gas barrier materials is shown, with tensile data of PET from previous work.[28,50] The elongation at break for the poly(ester-amide)s ranged from 1.4% (6G-2) to 342% (6G-5), with ultimate strength from 4 to 24 MPa (Figure 4 and Table S4). Tensile toughness values were also determined from the area under the stress–strain curve until failure and ranged from 0.11 to 60 MJ/m^3. Thus, the samples used in the study ranged from brittle and weak to ductile and strong.

For poly(ester-amide)s with molar masses of 10 – 20 kg/mol, increasing the number of methylene groups in y did not appreciably impact mechanical properties (Figure 4). 6G-3 and 6G-5 had slightly lower elastic moduli compared to poly(ester-amide)s with an even number of methylene groups (Figure S7). These results are in good agreement with previous studies of polyesters with even–odd effects.[51,52] Notably, compared to low molar mass of polymers, high molar mass versions of 6G-5 (27 kg/mol) and 6G-8 (32 kg/mol) showed outstanding mechanical properties competitive with PGA and PET and also showed strain hardening behavior (Figure 4 &

S8). After elongation, the enthalpy of melting for 6G-5 increased from 36 J/g to 65 J/g, consistent with strain-hardening caused by strain-induced crystallization during elongation (Figure S9).

To investigate the effect of alkyl chain lengths between amide groups (x) on mechanical properties, 2G-4, 4G-4, and 6G-4 were compared. 2G-4 with a high molar mass sample (31 kg/mol) showed ductility, with an elongation at break of 133% and an ultimate strength of 18 MPa (Figure 4B, 4D, and Table S4). Lower molar mass of 2G-4 (M_n = 17 kg/mol) was used to compare with 4G-4 (M_n = 11 kg/mol) and 6G-4 (M_n = 14 kg/mol), but the self-standing film of 2G-4 (M_n = 17 kg/mol) was hard to obtain due to its brittleness. As we increased alkyl chain lengths in x to 4 in 4G-4, a brittle film was obtained with an elongation at break of 3% and an ultimate strength of only 4 MPa (Figure 4B, 4D, and Table S4). By increasing x to 6 in 6G-4, elongation at break and ultimate strength were improved further to 39% and 10 MPa, respectively. Thus, longer alkyl chain lengths in x slightly increased the ultimate strength and strain. Overall, 6G-y samples at high molar mass are promising materials because they have broad thermal processing windows and comparable ultimate strain and strength to conventional gas barrier materials.

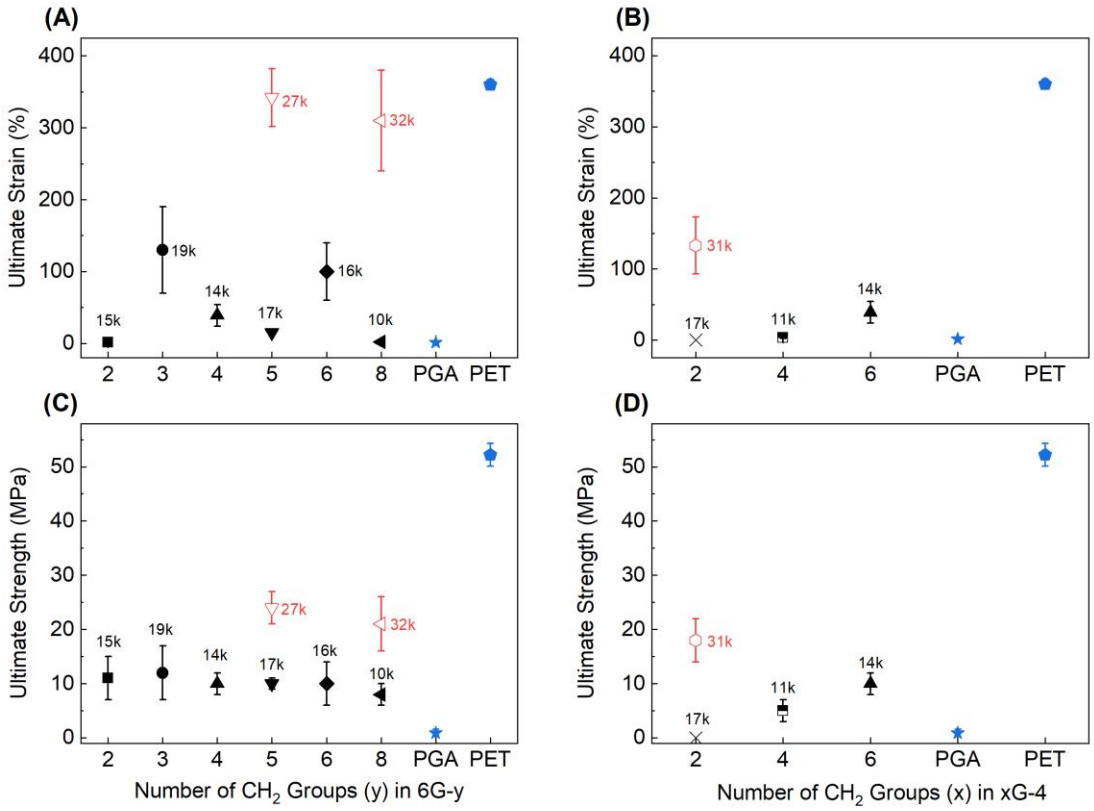

Figure 4. The effect of the number of methylene group on mechanical properties. Ultimate strain of (A) 6G-y, PGA (29 kg/mol), and PET (29 kg/mol)[50] and (B) xG-4, PGA (29 kg/mol), and PET (29 kg/mol)[50]. Ultimate strength of (C) 6G-y, PGA (29 kg/mol), and PET (29 kg/mol)[50] and (D) xG-4, PGA (29 kg/mol), and PET (29 kg/mol)[50]. The extension rate was 1 mm min^{-1} up to its break point.

Oxygen and water vapor permeability for selected poly(ester-amide)s

As a result of these competitive thermal and mechanical properties, poly(ester-amide)s of 6G-y with variable y were selected to investigate oxygen and water permeability. Oxygen and water vapor transmission rates of the films were measured and normalized by the thickness of the films and partial gas pressure to obtain gas permeability values. A summary of oxygen and water

vapor permeability is shown in Figure 5, along with commercially available polymers such as PGA, PET, and PLLA as benchmarks.[28,53–55]

Oxygen permeability of 6G-4 at 23 °C and 0% relative humidity (RH) was 45 cc·mil·m^{-2}·d^{-1}·atm^{-1} (Figure 5 & Table S5). As we increased the number of methylene groups between ester groups to 6 (6G-6) and 8 (6G-8), oxygen permeability values increased to 92 and 196 cc·mil·m^{-2}·d^{-1}·atm^{-1}, respectively. This is likely because of lower crystallinities due to the flexibility of alkyl chains in the repeat units. 6G-5 showed higher oxygen permeability compared to even number of poly(ester-amide)s such as 6G-4 and 6G-6. Although oxygen permeabilities of poly(ester-amide)s were higher than PGA, they were lower than those of PET and PLLA.

Water vapor permeabilities of poly(ester-amide)s were also explored at around 19 °C and 51% relative humidity (RH). The results showed 29 to 41 g·mil·m^{-2}·d^{-1}·kPa^{-1} of water vapor permeability, which are comparable to PLLA (Figure 5). There was no clear effect of the number of methylene group on water vapor permeability in this series.

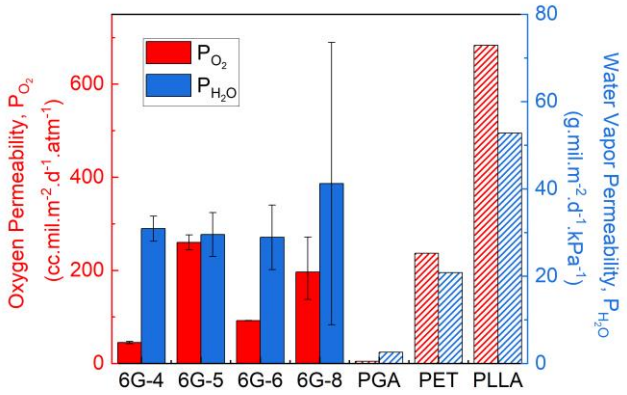

Figure 5. Oxygen and water vapor permeability of 6G-4, 6G-5, 6G-6, 6G-8, and reported PGA (86 kg/mol),[28] PET, [54 – 56] and PLLA (154 kg/mol).[53,54] The column bars show the average. The error bars for oxygen permeability and water vapor permeability show range for at least two replicates and standard deviation for five replicates, respectively.

Degradation Studies of poly(ester-amide)s

Vera et al. reported that 6G-4 is degradable in DI water at 70 °C and pH 2.3 medium at room temperature in previous studies.[37] We built upon this work by investigating hydrolysis of 6G-8 under various conditions, such as HCl (1 M), NaOH (1 M), and DI water, with monitoring by total organic carbon (TOC) analysis to quantify soluble hydrolysis products (Figure 6). In DI water at room temperature, leaching of organic compounds was less than 8% (Figure S10). At 50 °C, the hydrolysis products slightly increased compared to room temperature, but a plateau occurred at approximately 11% of TOC content. The hydrolysis rate significantly increased at 70 °C, and TOC content reached to 80% of carbon content expected for complete hydrolysis in 50 days. This rate was slower than previous studies of 6G-4, presumably because 6G-8 had more hydrophobic character than 6G-4.

We also performed hydrolysis experiments in aqueous acidic (1 M HCl) and basic (1 M NaOH) solutions at room temperature (Figure 6). In 1 M HCl, the rate of hydrolysis was much faster than in DI water at room temperature, and TOC content reached to 51% in 57 days. Hydrolysis in a basic solution (1 M NaOH) resulted in relatively linear growth of TOC content over time and complete degradation in 10 h (Figure 6). We observed near-complete disappearance of 6G-8 films after 5 h. Hydrolyzed products in NaOH solution (1 M in D_2O) were analyzed over time by ^{1}H NMR spectroscopy (Figure S11). Sebacate disodium salt and 6G were mostly observed after 8 h. Further hydrolysis of most amide groups gave rise to 1,6-diaminohexane and sodium glycolate salt in 12 d, suggesting that hydrolysis of ester groups was followed by that of amide groups. It was surprising that the hydrolysis rate of 6G-8 in NaOH (1 M) solution was much faster than that of poly(ester-amide)s derived from β-methyl-δ-valerolactone, as reported by Guptill et

al.[38] The faster kinetics observed for 6G-8 are presumably attributed to the higher hydrophilicity of the polymer and higher driving force for hydrolysis because the hydrolyzed product, 6G, can be stabilized by hydrogen bonding between N-H and O (Figure 1 & S3).

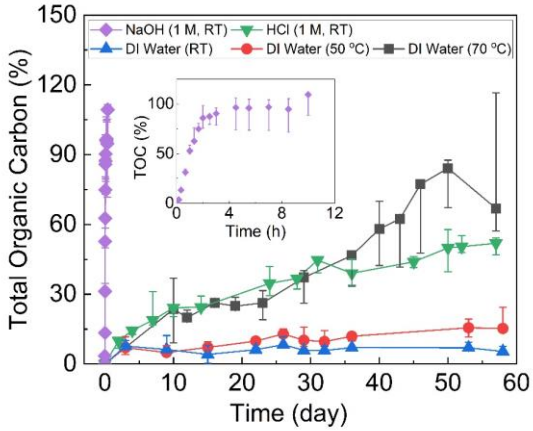

Figure 6. Hydrolytic degradation studies of 6G-8 in (A) DI water at room temperature, 50 °C, and 70 °C; 1 M HCl; and 1 M NaOH at room temperature. The total organic carbon data were obtained from total organic carbon content in the aqueous solutions divided by carbon content of 6G-8 films. The data points and error bars represent median and range for triplicate experiments, respectively.

Conclusion

We have demonstrated the synthesis and characterization of poly(ester-amide)s derived from glycolide. The monomers, diamidodiols, were prepared with perfect atom economy without any solvents or catalysts. Using renewable diamidodiols and aliphatic diacids, we synthesized various poly(ester-amide)s with M_n up to 32 kg/mol with different numbers of methylene groups to study structure–property relationships. Most polymers showed very wide thermal processing

windows ($T_{d,5\%} - T_m$) up to 236 °C. The melting and crystallization temperatures depended on the alkyl chain lengths of poly(ester-amide)s. Furthermore, mechanical properties of the 6G-y series at high molar mass were competitive with commercial gas barrier materials such as PGA and PET. Oxygen permeability of 6G-y series of the poly(ester-amide)s also outperformed PET and PLLA. The polymer films of 6G-8 were fully degradable in basic conditions (1 M NaOH) within 10 h to monomers based on TOC and NMR analysis. These results suggest that the 6G-y of poly(ester-amide)s at high molar mass are the most promising candidates for renewable, degradable and ductile gas barrier materials.

Author Information

Corresponding Author

Marc A. Hillmyer − Department of Chemistry, University of Minnesota, Minneapolis, Minnesota 55455-0431, United States; orcid.org/0000-0001-8255-3853; Email: hillmyer@umn.edu

Authors

Yoon-Jung Jang − Department of Chemistry, University of Minnesota, Minneapolis, Minnesota 55455-0431, United States; https://orcid.org/0000-0002-2592-1733

Leire Sangroniz − Department of Chemistry, University of Minnesota, Minneapolis, Minnesota 55455-0431, United States; https://orcid.org/0000-0003-0714-3154

Acknowledgement

This work was supported by National Science Foundation Center for Sustainable Polymers at the University of Minnesota, which is a National Science foundation-supported Center for Chemical Innovation (CHE-1901635) and Braskem. The authors thank Prof. Tom Hoye, Dr. Wui Yarn Chan and Dr. Christopher DeRosa at the University of Minnesota, Dr. Jay Werber at the University of Toronto, and Dr. Jason Clark at Braskem for helpful discussions. The authors also thank Kris Bednarchuk at Ametek and Donald Massey at Clemson University for assistance with measurements of oxygen transmission rate. The authors thank Dr. Victor Young Jr. at University of Minnesota and Steven Weigand at Argonne National Laboratory for X-ray experiments assistance. WAXS experiments were performed at the Sector 5 of the Advanced Photon Source at the DuPont-Northwestern-Dow Collaborative Access Team (DND-CAT), supported by E.I. DuPont de Nemours & Co., Northwestern University, and the U.S. DOE under contract no. DE-AC02-06CH11357.

Supporting Information

Experimental and instrumental details, Optimization of polymerization data, ^{1}H and ^{13}C NMR spectroscopy, size exclusion chromatography data, thermal gravimetric analysis data, differential scanning calorimetry data, X-ray experiments data, mechanical properties data, gas permeability data, hydrolytic degradation data.

Data Access Statement

All primary data files are available free of charge at 10.13020/2qz9-nj73.

References

(1) Wu, F.; Misra, M.; Mohanty, A. K. Challenges and New Opportunities on Barrier Performance of Biodegradable Polymers for Sustainable Packaging. *Prog. Polym. Sci.* **2021**, *117*, 101395. https://doi.org/10.1016/j.progpolymsci.2021.101395.

(2) Schneiderman, D. K.; Hillmyer, M. A. *50th Anniversary Perspective* : There Is a Great Future in Sustainable Polymers. *Macromolecules* **2017**, *50* (10), 3733–3749. https://doi.org/10.1021/acs.macromol.7b00293.

(3) Zekriardehani, S.; Jabarin, S. A.; Gidley, D. R.; Coleman, M. R. Effect of Chain Dynamics, Crystallinity, and Free Volume on the Barrier Properties of Poly(Ethylene Terephthalate) Biaxially Oriented Films. *Macromolecules* **2017**, *50* (7), 2845–2855. https://doi.org/10.1021/acs.macromol.7b00198.

(4) Lange, J.; Wyser, Y. Recent Innovations in Barrier Technologies for Plastic Packaging?A Review. *Packag. Technol. Sci.* **2003**, *16* (4), 149–158. https://doi.org/10.1002/pts.621.

(5) Maes, C.; Luyten, W.; Herremans, G.; Peeters, R.; Carleer, R.; Buntinx, M. Recent Updates on the Barrier Properties of Ethylene Vinyl Alcohol Copolymer (EVOH): A Review. *Polym. Rev.* **2018**, *58* (2), 209–246. https://doi.org/10.1080/15583724.2017.1394323.

(6) Lagaron, J. M.; Catalá, R.; Gavara, R. Structural Characteristics Defining High Barrier Properties in Polymeric Materials. *Mater. Sci. Technol.* **2004**, *20* (1), 1–7. https://doi.org/10.1179/026708304225010442.

(7) MacArthur, E. Beyond Plastic Waste. *Science* **2017**, *358* (6365), 843–843. https://doi.org/10.1126/science.aao6749.

(8) Rochman, C. M.; Browne, M. A.; Halpern, B. S.; Hentschel, B. T.; Hoh, E.; Karapanagioti, H. K.; Rios-Mendoza, L. M.; Takada, H.; Teh, S.; Thompson, R. C. Classify Plastic Waste as Hazardous. *Nature* **2013**, *494* (7436), 169–171. https://doi.org/10.1038/494169a.

(9) Geyer, R.; Jambeck, J. R.; Law, K. L. Production, Use, and Fate of All Plastics Ever Made. *Sci. Adv.* **2017**, *3* (7), e1700782. https://doi.org/10.1126/sciadv.1700782.

(10) Albertsson, A.-C.; Hakkarainen, M. Designed to Degrade. *Science* **2017**, *358* (6365), 872–873. https://doi.org/10.1126/science.aap8115.

(11) Hillmyer, M. A. The Promise of Plastics from Plants. *Science* **2017**, *358* (6365), 868–870. https://doi.org/10.1126/science.aao6711.

(12) Williams, C.; Hillmyer, M. Polymers from Renewable Resources: A Perspective for a Special Issue of Polymer Reviews. *Polym. Rev.* **2008**, *48* (1), 1–10. https://doi.org/10.1080/15583720701834133.

(13) Shaikh, S.; Yaqoob, M.; Aggarwal, P. An Overview of Biodegradable Packaging in Food Industry. *Curr. Res. Food Sci.* **2021**, *4*, 503–520. https://doi.org/10.1016/j.crfs.2021.07.005.

(14) Sousa, A. F.; Vilela, C.; Fonseca, A. C.; Matos, M.; Freire, C. S. R.; Gruter, G.-J. M.; Coelho, J. F. J.; Silvestre, A. J. D. Biobased Polyesters and Other Polymers from 2,5-Furandicarboxylic Acid: A Tribute to Furan Excellency. *Polym. Chem.* **2015**, *6* (33), 5961–5983. https://doi.org/10.1039/C5PY00686D.

(15) Yu, Z.; Zhou, J.; Cao, F.; Wen, B.; Zhu, X.; Wei, P. Chemosynthesis and Characterization of Fully Biomass-Based Copolymers of Ethylene Glycol, 2,5-Furandicarboxylic Acid, and Succinic Acid. *J. Appl. Polym. Sci.* **2013**, *130* (2), 1415–1420. https://doi.org/10.1002/app.39344.

(16) Li, C.; Jiang, T.; Wang, J.; Peng, S.; Wu, H.; Shen, J.; Guo, S.; Zhang, X.; Harkin-Jones, E. Enhancing the Oxygen-Barrier Properties of Polylactide by Tailoring the Arrangement of Crystalline Lamellae.

ACS Sustain. Chem. Eng. **2018**, *6* (5), 6247–6255. https://doi.org/10.1021/acssuschemeng.8b00026.
(17) Xie, L.; Xu, H.; Chen, J.-B.; Zhang, Z.-J.; Hsiao, B. S.; Zhong, G.-J.; Chen, J.; Li, Z.-M. From Nanofibrillar to Nanolaminar Poly(Butylene Succinate): Paving the Way to Robust Barrier and Mechanical Properties for Full-Biodegradable Poly(Lactic Acid) Films. *ACS Appl. Mater. Interfaces* **2015**, *7* (15), 8023–8032. https://doi.org/10.1021/acsami.5b00294.
(18) Vannini, M.; Marchese, P.; Celli, A.; Lorenzetti, C. Fully Biobased Poly(Propylene 2,5-Furandicarboxylate) for Packaging Applications: Excellent Barrier Properties as a Function of Crystallinity. *Green Chem.* **2015**, *17* (8), 4162–4166. https://doi.org/10.1039/C5GC00991J.
(19) Fernandes Nassar, S.; Delpouve, N.; Sollogoub, C.; Guinault, A.; Stoclet, G.; Régnier, G.; Domenek, S. Impact of Nanoconfinement on Polylactide Crystallization and Gas Barrier Properties. *ACS Appl. Mater. Interfaces* **2020**, *12* (8), 9953–9965. https://doi.org/10.1021/acsami.9b21391.
(20) Xie, H.; Wu, L.; Li, B.-G.; Dubois, P. Modification of Poly(Ethylene 2,5-Furandicarboxylate) with Biobased 1,5-Pentanediol: Significantly Toughened Copolyesters Retaining High Tensile Strength and O_2 Barrier Property. *Biomacromolecules* **2019**, *20* (1), 353–364. https://doi.org/10.1021/acs.biomac.8b01495.
(21) Murcia Valderrama, M. A.; van Putten, R.-J.; Gruter, G.-J. M. PLGA Barrier Materials from CO_2. The Influence of Lactide Co-Monomer on Glycolic Acid Polyesters. *ACS Appl. Polym. Mater.* **2020**, *2* (7), 2706–2718. https://doi.org/10.1021/acsapm.0c00315.
(22) Drieskens, M.; Peeters, R.; Mullens, J.; Franco, D.; Lemstra, P. J.; Hristova-Bogaerds, D. G. Structure versus Properties Relationship of Poly(Lactic Acid). I. Effect of Crystallinity on Barrier Properties: Structure Vs. Barrier Properties of PLA. *J. Polym. Sci. Part B Polym. Phys.* **2009**, *47* (22), 2247–2258. https://doi.org/10.1002/polb.21822.
(23) Sinha Ray, S.; Okamoto, K.; Okamoto, M. Structure−Property Relationship in Biodegradable Poly(Butylene Succinate)/Layered Silicate Nanocomposites. *Macromolecules* **2003**, *36* (7), 2355–2367. https://doi.org/10.1021/ma021728y.
(24) Long, Y.; Zhang, R.; Huang, J.; Wang, J.; Jiang, Y.; Hu, G.; Yang, J.; Zhu, J. Tensile Property Balanced and Gas Barrier Improved Poly(Lactic Acid) by Blending with Biobased Poly(Butylene 2,5-Furan Dicarboxylate). *ACS Sustain. Chem. Eng.* **2017**, *5* (10), 9244–9253. https://doi.org/10.1021/acssuschemeng.7b02196.
(25) Yamane, K.; Sato, H.; Ichikawa, Y.; Sunagawa, K.; Shigaki, Y. Development of an Industrial Production Technology for High-Molecular-Weight Polyglycolic Acid. *Polym. J.* **2014**, *46* (11), 769–775. https://doi.org/10.1038/pj.2014.69.
(26) Samantaray, P. K.; Little, A.; Haddleton, D. M.; McNally, T.; Tan, B.; Sun, Z.; Huang, W.; Ji, Y.; Wan, C. Poly(Glycolic Acid) (PGA): A Versatile Building Block Expanding High Performance and Sustainable Bioplastic Applications. *Green Chem.* **2020**, *22* (13), 4055–4081. https://doi.org/10.1039/D0GC01394C.
(27) Yu, C.; Bao, J.; Xie, Q.; Shan, G.; Bao, Y.; Pan, P. Crystallization Behavior and Crystalline Structural Changes of Poly(Glycolic Acid) Investigated via Temperature-Variable WAXD and FTIR Analysis. *CrystEngComm* **2016**, *18* (40), 7894–7902. https://doi.org/10.1039/C6CE01623E.
(28) Altay, E.; Jang, Y.-J.; Kua, X. Q.; Hillmyer, M. A. Synthesis, Microstructure, and Properties of High-Molar-Mass Polyglycolide Copolymers with Isolated Methyl Defects. *Biomacromolecules* **2021**, *22* (6), 2532–2543. https://doi.org/10.1021/acs.biomac.1c00269.
(29) Rodriguez-Galan, A.; Franco, L.; Puiggali, J. Degradable Poly(Ester Amide)s for Biomedical Applications. *Polymers* **2010**, *3* (1), 65–99. https://doi.org/10.3390/polym3010065.
(30) Winnacker, M.; Rieger, B. Poly(Ester Amide)s: Recent Insights into Synthesis, Stability and Biomedical Applications. *Polym. Chem.* **2016**, *7* (46), 7039–7046. https://doi.org/10.1039/C6PY01783E.

(31) Ghosal, K.; Latha, M. S.; Thomas, S. Poly(Ester Amides) (PEAs) – Scaffold for Tissue Engineering Applications. *Eur. Polym. J.* **2014**, *60*, 58–68. https://doi.org/10.1016/j.eurpolymj.2014.08.006.
(32) Díaz, A.; Katsarava, R.; Puiggalí, J. Synthesis, Properties and Applications of Biodegradable Polymers Derived from Diols and Dicarboxylic Acids: From Polyesters to Poly(Ester Amide)s. *Int. J. Mol. Sci.* **2014**, *15* (5), 7064–7123. https://doi.org/10.3390/ijms15057064.
(33) Gao, H.; Bai, Y.; Liu, H.; He, J. Mechanical and Gas Barrier Properties of Structurally Enhanced Poly(Ethylene Terephthalate) by Introducing 1,6-Hexylenediamine Unit. *Ind. Eng. Chem. Res.* **2019**, *58* (47), 21872–21880. https://doi.org/10.1021/acs.iecr.9b04953.
(34) Báez, J. E.; Ramírez, D.; Valentín, J. L.; Marcos-Fernández, Á. Biodegradable Poly(Ester–Urethane–Amide)s Based on Poly(ε-Caprolactone) and Diamide–Diol Chain Extenders with Crystalline Hard Segments. Synthesis and Characterization. *Macromolecules* **2012**, *45* (17), 6966–6980. https://doi.org/10.1021/ma300990s.
(35) Lips, P. A. M.; Broos, R.; van Heeringen, M. J. M.; Dijkstra, P. J.; Feijen, J. Incorporation of Different Crystallizable Amide Blocks in Segmented Poly(Ester Amide)s. *Polymer* **2005**, *46* (19), 7834–7842. https://doi.org/10.1016/j.polymer.2005.07.009.
(36) Stapert, H. R.; Dijkstra, P. J.; Feijen, J. Synthesis and Characterization of Aliphatic Poly(Esteramide)s Containing Symmetrical Bisamide Blocks. *Macromol. Symp.* **1998**, *130* (1), 91–102. https://doi.org/10.1002/masy.19981300109.
(37) Vera, M.; Admetlla, M.; Rodríguez-Galán, A.; Puiggalí, J. Synthesis, Characterization and Degradation Studies on the Series of Sequential Poly(Ester Amide)s Derived from Glycolic Acid, 1,6-Hexanediamine and Aliphatic Dicarboxylic Acids. *Polym. Degrad. Stab.* **2005**, *89* (1), 21–32. https://doi.org/10.1016/j.polymdegradstab.2004.12.020.
(38) Guptill, D. M.; Chinta, B. S.; Kaicharla, T.; Xu, S.; Hoye, T. R. β-Methyl-δ-Valerolactone-Containing Thermoplastic Poly(Ester-Amide)s: Synthesis, Mechanical Properties, and Degradation Behavior. *Polym. Chem.* **2021**, *12* (9), 1310–1316. https://doi.org/10.1039/D1PY00040C.
(39) Krook, M.; Albertsson, A.-C.; Gedde, U. W.; Hedenqvist, M. S. Barrier and Mechanical Properties of Montmorillonite/Polyesteramide Nanocomposites. *Polym. Eng. Sci.* **2002**, *42* (6), 1238–1246. https://doi.org/10.1002/pen.11027.
(40) Rader, C.; Weder, C.; Marti, R. Biobased Polyester-Amide/Cellulose Nanocrystal Nanocomposites for Food Packaging. *Macromol. Mater. Eng.* **2021**, *306* (3), 2000668. https://doi.org/10.1002/mame.202000668.
(41) Murase, S. K.; Franco, L.; del Valle, L. J.; Puiggalí, J. Synthesis and Characterization of Poly(Ester Amides)s with a Variable Ratio of Branched Odd Diamide Units. *J. Appl. Polym. Sci.* **2014**, *131* (7), n/a-n/a. https://doi.org/10.1002/app.40102.
(42) Murase, S.; del Valle, L.; Puiggalí, J. Electrospun Scaffolds from Low Molecular Weight Poly(Ester Amide)s Based on Glycolic Acid, Adipic Acid and Odd or Even Diamines. *Fibers* **2015**, *3* (4), 151–172. https://doi.org/10.3390/fib3020151.
(43) Zamudio Rivera, L. S.; Carrillo, L.; Mancilla, T. SYNTHESIS AND CHARACTERIZATION OF N-ALKYL HYDROXYACETAMIDES. *Org. Prep. Proced. Int.* **2000**, *32* (1), 84–88. https://doi.org/10.1080/00304940009356751.
(44) Casas, M. T.; Puiggalí, J. Crystalline Structure of Sequential Poly(Ester Amide)s Derived from Glycolic Acid, 1,6-Hexanediamine, and Even Aliphatic Dicarboxylic Acids. *J. Polym. Sci. Part B Polym. Phys.* **2009**, *47* (2), 194–206. https://doi.org/10.1002/polb.21630.
(45) CSIRO Molecular Science, Bag 10, Clayton South MDC, Vic 3169, Australia; Gunatillake, P. Biodegradable Synthetic Polymers for Tissue Engineering. *Eur. Cell. Mater.* **2003**, *5*, 1–16. https://doi.org/10.22203/eCM.v005a01.
(46) Wang, L.; Li, G.; Deng, Y. Diamine Biosynthesis: Research Progress and Application Prospects. *Appl. Environ. Microbiol.* **2020**, *86* (23). https://doi.org/10.1128/AEM.01972-20.

(47) Sangroniz, L.; Jang, Y.-J.; Hillmyer, M. A.; Müller, A. J. The Role of Intermolecular Interactions on Melt Memory and Thermal Fractionation of Semicrystalline Polymers. *J. Chem. Phys.* **2022**, *156* (14), 144902. https://doi.org/10.1063/5.0087782.
(48) Stempfle, F.; Ortmann, P.; Mecking, S. Long-Chain Aliphatic Polymers To Bridge the Gap between Semicrystalline Polyolefins and Traditional Polycondensates. *Chem. Rev.* **2016**, *116* (7), 4597–4641. https://doi.org/10.1021/acs.chemrev.5b00705.
(49) Nomura, K.; Binti Awang, N. W. Synthesis of Bio-Based Aliphatic Polyesters from Plant Oils by Efficient Molecular Catalysis: A Selected Survey from Recent Reports. *ACS Sustain. Chem. Eng.* **2021**, *9* (16), 5486–5505. https://doi.org/10.1021/acssuschemeng.1c00493.
(50) Kim, H. J.; Peng, X.; Shin, Y.; Hillmyer, M. A.; Ellison, C. J. Blend Miscibility of Poly(Ethylene Terephthalate) and Aromatic Polyesters from Salicylic Acid. *J. Phys. Chem. B* **2021**, *125* (1), 450–460. https://doi.org/10.1021/acs.jpcb.0c09322.
(51) Lu, J.; Wu, L.; Li, B.-G. High Molecular Weight Polyesters Derived from Biobased 1,5-Pentanediol and a Variety of Aliphatic Diacids: Synthesis, Characterization, and Thermo-Mechanical Properties. *ACS Sustain. Chem. Eng.* **2017**, *5* (7), 6159–6166. https://doi.org/10.1021/acssuschemeng.7b01050.
(52) Zhou, C.; Wei, Z.; Yu, Y.; Shao, S.; Leng, X.; Wang, Y.; Li, Y. Biobased Long-Chain Aliphatic Polyesters of 1,12-Dodecanedioic Acid with a Variety of Diols: Odd-Even Effect and Mechanical Properties. *Mater. Today Commun.* **2019**, *19*, 450–458. https://doi.org/10.1016/j.mtcomm.2019.05.005.
(53) Sangroniz, A.; Chaos, A.; Iriarte, M.; del Río, J.; Sarasua, J.-R.; Etxeberria, A. Influence of the Rigid Amorphous Fraction and Crystallinity on Polylactide Transport Properties. *Macromolecules* **2018**, *51* (11), 3923–3931. https://doi.org/10.1021/acs.macromol.8b00833.
(54) Sangroniz, A.; Zhu, J.-B.; Tang, X.; Etxeberria, A.; Chen, E. Y.-X.; Sardon, H. Packaging Materials with Desired Mechanical and Barrier Properties and Full Chemical Recyclability. *Nat. Commun.* **2019**, *10* (1), 3559. https://doi.org/10.1038/s41467-019-11525-x.
(55) Sangroniz, L.; Ruiz, J. L.; Sangroniz, A.; Fernández, M.; Etxeberria, A.; Müller, A. J.; Santamaria, A. Polyethylene Terephthalate/Low Density Polyethylene/Titanium Dioxide Blend Nanocomposites: Morphology, Crystallinity, Rheology, and Transport Properties. *J. Appl. Polym. Sci.* **2019**, *136* (4), 46986. https://doi.org/10.1002/app.46986.
(56) Molar mass of PET was not reported in previous work, but the PET was from Brilen (Novapet CR, Barbastro, Spain) and its intrinsic viscosity was 0.80 dlg^{-1} in m-cresol.